



Searches for R-parity violating Supersymmetry at LEP II

The ALEPH Collaboration

Abstract

Searches for pair-production of Supersymmetric particles under the assumption that R-parity is not conserved have been performed using the data collected by ALEPH at centre-of-mass energies of 130-172 GeV. The results for a dominant R-parity violating coupling $LL\bar{E}$, for which the observed candidate events in the data are in agreement with the Standard Model expectation, translate into lower limits on the mass of charginos, neutralinos, sleptons, sneutrinos and squarks. We also give preliminary results on the search for charginos, sleptons and sneutrinos via a dominant $LQ\bar{D}$ coupling, and discuss the implications of these results on the R-parity violating interpretations of the recently reported excess of high Q^2 events at HERA, and the ALEPH four jet anomaly.

Submitted to the 1997 EPS-HEP conference, Jerusalem.

The ALEPH Collaboration

R. Barate, D. Buskulic, D. Decamp, P. Ghez, C. Goy, J.-P. Lees, A. Lucotte, M.-N. Minard, J.-Y. Nief, B. Pietrzyk

Laboratoire de Physique des Particules (LAPP), IN²P³-CNRS, 74019 Annecy-le-Vieux Cedex, France

M.P. Casado, M. Chmeissani, P. Comas, J.M. Crespo, M. Delfino, E. Fernandez, M. Fernandez-Bosman, Ll. Garrido,¹⁵ A. Juste, M. Martinez, G. Merino, R. Miquel, Ll.M. Mir, C. Padilla, I.C. Park, A. Pascual, J.A. Perlas, I. Riu, F. Sanchez, F. Teubert

Institut de Física d'Altes Energies, Universitat Autònoma de Barcelona, 08193 Bellaterra (Barcelona), Spain⁷

A. Colaleo, D. Creanza, M. de Palma, G. Gelao, G. Iaselli, G. Maggi, M. Maggi, N. Marinelli, S. Nuzzo, A. Ranieri, G. Raso, F. Ruggieri, G. Selvaggi, L. Silvestris, P. Tempesta, A. Tricomi,³ G. Zito

Dipartimento di Fisica, INFN Sezione di Bari, 70126 Bari, Italy

X. Huang, J. Lin, Q. Ouyang, T. Wang, Y. Xie, R. Xu, S. Xue, J. Zhang, L. Zhang, W. Zhao

Institute of High-Energy Physics, Academia Sinica, Beijing, The People's Republic of China⁸

D. Abbaneo, R. Alemany, A.O. Bazarko,¹ U. Becker, P. Bright-Thomas, M. Cattaneo, F. Cerutti, G. Dissertori, H. Drevermann, R.W. Forty, M. Frank, R. Hagelberg, J.B. Hansen, J. Harvey, P. Janot, B. Jost, E. Kneringer, J. Knobloch, I. Lehraus, P. Mato, A. Minten, L. Moneta, A. Pacheco, J.-F. Puztaszeri,²⁰ F. Ranjard, G. Rizzo, L. Rolandi, D. Rousseau, D. Schlatter, M. Schmitt, O. Schneider, W. Tejessy, I.R. Tomalin, H. Wachsmuth, A. Wagner²¹

European Laboratory for Particle Physics (CERN), 1211 Geneva 23, Switzerland

Z. Ajaltouni, A. Barrès, C. Boyer, A. Falvard, C. Ferdi, P. Gay, C. Guicheney, P. Henrard, J. Jousset, B. Michel, S. Monteil, J.-C. Montret, D. Pallin, P. Perret, F. Podlyski, J. Proriot, P. Rosnet, J.-M. Rossignol

Laboratoire de Physique Corpusculaire, Université Blaise Pascal, IN²P³-CNRS, Clermont-Ferrand, 63177 Aubière, France

T. Fearnley, J.D. Hansen, J.R. Hansen, P.H. Hansen, B.S. Nilsson, B. Rensch, A. Wäänänen

Niels Bohr Institute, 2100 Copenhagen, Denmark⁹

G. Daskalakis, A. Kyriakis, C. Markou, E. Simopoulou, A. Vayaki

Nuclear Research Center Demokritos (NRCD), Athens, Greece

A. Blondel, J.C. Brient, F. Machefert, A. Rougé, M. Rumpf, A. Valassi,⁶ H. Videau

Laboratoire de Physique Nucléaire et des Hautes Energies, Ecole Polytechnique, IN²P³-CNRS, 91128 Palaiseau Cedex, France

E. Focardi, G. Parrini, K. Zachariadou

Dipartimento di Fisica, Università di Firenze, INFN Sezione di Firenze, 50125 Firenze, Italy

R. Cavanaugh, M. Corden, C. Georgiopoulos, T. Huehn, D.E. Jaffe

Supercomputer Computations Research Institute, Florida State University, Tallahassee, FL 32306-4052, USA^{13,14}

A. Antonelli, G. Bencivenni, G. Bologna,⁴ F. Bossi, P. Campana, G. Capon, D. Casper, V. Chiarella, G. Felici, P. Laurelli, G. Mannocchi,⁵ F. Murtas, G.P. Murtas, L. Passalacqua, M. Pepe-Altarelli

Laboratori Nazionali dell'INFN (LNF-INFN), 00044 Frascati, Italy

L. Curtis, S.J. Dorris, A.W. Halley, I.G. Knowles, J.G. Lynch, V. O'Shea, C. Raine, J.M. Scarr, K. Smith, P. Teixeira-Dias, A.S. Thompson, E. Thomson, F. Thomson, R.M. Turnbull

Department of Physics and Astronomy, University of Glasgow, Glasgow G12 8QQ, United Kingdom¹⁰

O. Buchmüller, S. Dhamotharan, C. Geweniger, G. Graefe, P. Hanke, G. Hansper, V. Hepp, E.E. Kluge,

- A. Putzer, J. Sommer, K. Tittel, S. Werner, M. Wunsch
*Institut für Hochenergiephysik, Universität Heidelberg, 69120 Heidelberg, Fed. Rep. of Germany*¹⁶
- R. Beuselinck, D.M. Binnie, W. Cameron, P.J. Dornan, M. Girone, S. Goodsir, E.B. Martin, P. Morawitz, A. Moutoussi, J. Nash, J.K. Sedgbeer, P. Spagnolo, A.M. Stacey, M.D. Williams
*Department of Physics, Imperial College, London SW7 2BZ, United Kingdom*¹⁰
- V.M. Ghete, P. Girtler, D. Kuhn, G. Rudolph
*Institut für Experimentalphysik, Universität Innsbruck, 6020 Innsbruck, Austria*¹⁸
- A.P. Betteridge, C.K. Bowdery, P. Colrain, G. Crawford, A.J. Finch, F. Foster, G. Hughes, R.W.L. Jones, T. Sloan, E.P. Whelan, M.I. Williams
*Department of Physics, University of Lancaster, Lancaster LA1 4YB, United Kingdom*¹⁰
- C. Hoffmann, K. Jakobs, K. Kleinknecht, G. Quast, B. Renk, E. Rohne, H.-G. Sander, P. van Gemmeren, C. Zeitnitz
*Institut für Physik, Universität Mainz, 55099 Mainz, Fed. Rep. of Germany*¹⁶
- J.J. Aubert, C. Benchouk, A. Bonissent, G. Bujosa, J. Carr, P. Coyle, C. Diaconu, A. Ealet, D. Fouchez, N. Konstantinidis, O. Leroy, F. Motsch, P. Payre, M. Talby, A. Sadouki, M. Thulasidas, A. Tilquin, K. Trabelsi
Centre de Physique des Particules, Faculté des Sciences de Luminy, IN²P³-CNRS, 13288 Marseille, France
- M. Aleppo, M. Antonelli, F. Ragusa¹²
Dipartimento di Fisica, Università di Milano e INFN Sezione di Milano, 20133 Milano, Italy.
- R. Berlich, W. Blum, V. Büscher, H. Dietl, G. Ganis, C. Gotzhein, H. Kroha, G. Lütjens, G. Lutz, W. Männer, H.-G. Moser, R. Richter, A. Rosado-Schlosser, S. Schael, R. Settles, H. Seywerd, R. St. Denis, H. Stenzel, W. Wiedenmann, G. Wolf
*Max-Planck-Institut für Physik, Werner-Heisenberg-Institut, 80805 München, Fed. Rep. of Germany*¹⁶
- J. Boucrot, O. Callot,¹² S. Chen, A. Cordier, M. Davier, L. Duflot, J.-F. Grivaz, Ph. Heusse, A. Höcker, A. Jacholkowska, M. Jacquet, D.W. Kim,² F. Le Diberder, J. Lefrançois, A.-M. Lutz, I. Nikolic, M.-H. Schune, L. Serin, S. Simion, E. Tournefier, J.-J. Veillet, I. Videau, D. Zerwas
Laboratoire de l'Accélérateur Linéaire, Université de Paris-Sud, IN²P³-CNRS, 91405 Orsay Cedex, France
- P. Azzurri, G. Bagliesi, S. Bettarini, C. Bozzi, G. Calderini, V. Ciulli, R. Dell'Orso, R. Fantechi, I. Ferrante, A. Giassi, A. Gregorio, F. Ligabue, A. Lusiani, P.S. Marrocchesi, A. Messineo, F. Palla, G. Sanguinetti, A. Sciabà, G. Sguazzoni, J. Steinberger, R. Tenchini, C. Vannini, A. Venturi, P.G. Verdini
Dipartimento di Fisica dell'Università, INFN Sezione di Pisa, e Scuola Normale Superiore, 56010 Pisa, Italy
- G.A. Blair, L.M. Bryant, J.T. Chambers, Y. Gao, M.G. Green, T. Medcalf, P. Perrodo, J.A. Strong, J.H. von Wimmersperg-Toeller
*Department of Physics, Royal Holloway & Bedford New College, University of London, Surrey TW20 OEX, United Kingdom*¹⁰
- D.R. Botterill, R.W. Clift, T.R. Edgecock, S. Haywood, P. Maley, P.R. Norton, J.C. Thompson, A.E. Wright
*Particle Physics Dept., Rutherford Appleton Laboratory, Chilton, Didcot, Oxon OX11 0QX, United Kingdom*¹⁰
- B. Bloch-Devaux, P. Colas, B. Fabbro, W. Kozanecki, E. Lançon, M.C. Lemaire, E. Locci, P. Perez, J. Rander, J.-F. Renardy, A. Rosowsky, A. Roussarie, J.-P. Schuller, J. Schwinding, A. Trabelsi, B. Vallage
*CEA, DAPNIA/Service de Physique des Particules, CE-Saclay, 91191 Gif-sur-Yvette Cedex, France*¹⁷
- S.N. Black, J.H. Dann, H.Y. Kim, A.M. Litke, M.A. McNeil, G. Taylor
*Institute for Particle Physics, University of California at Santa Cruz, Santa Cruz, CA 95064, USA*¹⁹

C.N. Booth, R. Boswell, C.A.J. Brew, S. Cartwright, F. Combley, M.S. Kelly, M. Lehto, W.M. Newton, J. Reeve, L.F. Thompson

*Department of Physics, University of Sheffield, Sheffield S3 7RH, United Kingdom*¹⁰

K. Affholderbach, A. Böhler, S. Brandt, G. Cowan, J. Foss, C. Grupen, G. Lutters, P. Saraiva, L. Smolik, F. Stephan

*Fachbereich Physik, Universität Siegen, 57068 Siegen, Fed. Rep. of Germany*¹⁶

M. Apollonio, L. Bosisio, R. Della Marina, G. Giannini, B. Gobbo, G. Musolino

Dipartimento di Fisica, Università di Trieste e INFN Sezione di Trieste, 34127 Trieste, Italy

J. Putz, J. Rothberg, S. Wasserbaech, R.W. Williams

Experimental Elementary Particle Physics, University of Washington, WA 98195 Seattle, U.S.A.

S.R. Armstrong, E. Charles, P. Elmer, D.P.S. Ferguson, S. González, T.C. Greening, O.J. Hayes, H. Hu, S. Jin, P.A. McNamara III, J.M. Nachtman, J. Nielsen, W. Orejudos, Y.B. Pan, Y. Saadi, I.J. Scott, J. Walsh, Sau Lan Wu, X. Wu, J.M. Yamartino, G. Zoernig

*Department of Physics, University of Wisconsin, Madison, WI 53706, USA*¹¹

¹Now at Princeton University, Princeton, NJ 08544, U.S.A.

²Permanent address: Kangnung National University, Kangnung, Korea.

³Also at Dipartimento di Fisica, INFN Sezione di Catania, Catania, Italy.

⁴Also Istituto di Fisica Generale, Università di Torino, Torino, Italy.

⁵Also Istituto di Cosmo-Geofisica del C.N.R., Torino, Italy.

⁶Supported by the Commission of the European Communities, contract ERBCHBICT941234.

⁷Supported by CICYT, Spain.

⁸Supported by the National Science Foundation of China.

⁹Supported by the Danish Natural Science Research Council.

¹⁰Supported by the UK Particle Physics and Astronomy Research Council.

¹¹Supported by the US Department of Energy, grant DE-FG0295-ER40896.

¹²Also at CERN, 1211 Geneva 23, Switzerland.

¹³Supported by the US Department of Energy, contract DE-FG05-92ER40742.

¹⁴Supported by the US Department of Energy, contract DE-FC05-85ER250000.

¹⁵Permanent address: Universitat de Barcelona, 08208 Barcelona, Spain.

¹⁶Supported by the Bundesministerium für Bildung, Wissenschaft, Forschung und Technologie, Fed. Rep. of Germany.

¹⁷Supported by the Direction des Sciences de la Matière, C.E.A.

¹⁸Supported by Fonds zur Förderung der wissenschaftlichen Forschung, Austria.

¹⁹Supported by the US Department of Energy, grant DE-FG03-92ER40689.

²⁰Now at School of Operations Research and Industrial Engineering, Cornell University, Ithaca, NY 14853-3801, U.S.A.

²¹Now at Schweizerischer Bankverein, Basel, Switzerland.

1 Introduction

The minimal supersymmetric extension of the Standard Model (SM) requires that the SM particle content is doubled and an extra Higgs $SU(2)_L$ doublet is added. The most general interactions of these particles invariant under the $SU(3)_c \times SU(2)_L \times U(1)_Y$ gauge symmetry are those of the Minimal Supersymmetric Standard Model (MSSM) [1] plus the additional superpotential terms [2]

$$W_{R_p} = \lambda_{ijk} L_i L_j \bar{E}_k + \lambda'_{ijk} L_i Q_j \bar{D}_k + \lambda''_{ijk} \bar{U}_i \bar{D}_j \bar{D}_k. \quad (1)$$

Here L (Q) are the lepton (quark) doublet superfields, and \bar{D} , \bar{U} (\bar{E}) are the down-like and up-like quark (lepton) singlet superfields, respectively; $\lambda, \lambda', \lambda''$ are Yukawa couplings, and $i, j, k = 1..3$ are generation indices. The simultaneous presence of the last two terms leads to rapid proton decay, and the solution of this problem in the MSSM is to exclude all terms in Eq.(1) by imposing R-parity ($R_p = -1^{3B+L+2S}$)¹, a discrete multiplicative symmetry. This solution is not unique, and a number of models [3, 4, 5] predict only a subset of the terms in (1), thus protecting the proton from decay. These alternative solutions are denoted ‘‘R-parity violation’’.

If R-parity is violated, the Lightest Supersymmetric Particle (LSP) is not stable and decays to SM particles. Consequently the signatures are very different from the classic missing energy signatures of R-parity conserving models. This paper reports the results of searches for pair-produced supersymmetric particles at centre-of-mass energies from 130 to 172 GeV in the data recorded by the ALEPH detector in 1995-1996 assuming that R-parity is violated through either a dominant $LL\bar{E}$ coupling, or a dominant $LQ\bar{D}$ coupling. These results complement the previously reported ALEPH searches for R-parity violating Supersymmetry (SUSY) at LEP 1 energies [6], and the searches for charginos and neutralinos at energies up to 136 GeV [7].

We make two simplifying assumptions throughout our analysis:

- Only one of the three terms in Eq.(1) is non-zero. In this paper we limit ourselves to signals arising from the $LL\bar{E}$ or $LQ\bar{D}$ couplings. When we translate our results into limits, we also assume that only one of the possible nine λ_{ijk} couplings² (or one of the possible 27 λ'_{ijk} couplings) is non-zero, but note that the search analyses are not restricted to this assumption. In order to be conservative, we choose the coupling which gives the most conservative exclusion limit.
- The lifetime of the LSP is negligible; i.e. the mean free path of flight is less than ~ 1 cm.

The second assumption restricts our sensitivity in λ , which we can probe down to $\lambda \gtrsim 10^{-7}$, well below existing limits from low energy constraints. We make no assumption on the nature of the LSP for the $LL\bar{E}$ operator.

We briefly outline our paper: after reviewing the phenomenology of R-parity violating SUSY models in Section 2, we present the search analyses and their confrontation with data in Section 3. The results are interpreted in terms of limits for a dominant $LL\bar{E}$ and $LQ\bar{D}$ coupling in Sections 4 and 5, respectively. We comment on the relevance of our results on

¹Here B denotes the baryon number, L the lepton number and S the spin of a field.

²The λ_{ijk} coupling is antisymmetric in the i and j indices, hence $j > i$.

Coupling	R-parity violating Decay Mode
$LL\bar{E}$ (λ_{ijk})	χ^+ \rightarrow $\nu_i\nu_j l_k^+$, $l_i^+ l_j^+ l_k^-$, $l_i^+ \nu_j \nu_k$, $\nu_i l_j^+ \nu_k$
	χ \rightarrow $\bar{\nu}_i l_j^+ l_k^-$, $\bar{\nu}_j l_k^+ l_i^-$, $\nu_i l_j^- l_k^+$, $\nu_j l_i^- l_k^+$
	\tilde{l}_{iL}^- \rightarrow $\nu_j l_k^-$
	\tilde{l}_{kR}^- \rightarrow $\nu_i l_j^-$, $\nu_j l_i^-$
	$\tilde{\nu}_i$ \rightarrow $l_j^- l_k^+$
$LQ\bar{D}$ (λ'_{ijk})	χ \rightarrow $l_i^- u_j d_k$, $l_i^+ \bar{u}_j d_k$, $\nu_i d_j d_k$, $\bar{\nu}_i d_j d_k$
	\tilde{l}_{iL}^- \rightarrow $\bar{u}_j d_k$
	$\tilde{\nu}_{iL}$ \rightarrow $d_j \bar{d}_k$

Table 1: *R-parity violating decay modes relevant to this analysis. Here i, j, k are generation indices. For example, the electron sneutrino can decay via the coupling λ_{132} to: $\tilde{\nu}_e \rightarrow \tau^- \mu^+$.*

the R-parity violating interpretations [8] of the excess of high Q^2 events in positron-proton collisions recently reported by the H1 and the ZEUS Collaboration [9], and the R-parity violating interpretation [10] of the ALEPH four jet events in Section 6, and finally conclude.

2 Phenomenology

Within minimal Supersymmetry all SM fermions have scalar SUSY partners: the sleptons, sneutrinos and squarks. The SUSY equivalent of the gauge and Higgs bosons are the charginos and neutralinos, which are the mass eigenstates of the $(\tilde{W}^+, \tilde{H}^+)$ and $(\tilde{\gamma}, \tilde{Z}, \tilde{H}_1^0, \tilde{H}_2^0)$ fields, respectively. The lightest SUSY particle takes a special role in R-parity conserving models: it must be stable [11]. Cosmological arguments [12] then require it to be neutral, and the only possible LSP candidates are the neutralino and the sneutrino. If R-parity is violated, the LSP can decay to SM particles, and the above cosmological arguments do not apply. Good LSP candidates are the neutralino, the chargino, the sleptons, the sneutrinos and the stop or sbottom³.

The production cross sections do not depend on the size of the R-parity violating Yukawa coupling λ , since we consider the pair-production of sparticles. Sparticles can decay directly to SM particles via the R-parity violating Yukawa coupling λ_{ijk} or λ'_{ijk} . The allowed decays are summarised in Table 1, which are throughout referred to as the “direct” decay modes. Furthermore sparticles can decay indirectly to the LSP via the R-parity conserving couplings, and the LSP can subsequently decay violating R-parity. These decays will be referred to as the “indirect” decay modes. The branching ratios of the direct to indirect decay modes depend explicitly on the *a priori* unknown size of the Yukawa coupling λ , the masses and couplings of the decaying sparticle and the lighter SUSY states, and the nature of the LSP [13]. In order to be as model independent as possible, we consider all topologies arising from both classes of decays in the subsequent analyses. For a dominant $LQ\bar{D}$ coupling only results on indirect chargino decays and direct slepton/sneutrino decays are presented in this paper.

Following the above terminology, the lightest neutralino can decay *directly* to two leptons

³We do not consider stop or sbottom LSPs for a dominant λ_{ijk} coupling, since they cannot decay directly via the purely leptonic $LL\bar{E}$ operator, and would instead have to undergo a slow 4-body decay, acquire a substantial lifetime, and fall outside our assumption of negligible lifetime.

and a neutrino for a dominant $LL\bar{E}$ coupling, (either via 2-body decays to lighter sleptons or sneutrinos, or via a 3-body decay), or to a lepton or a neutrino and two jets for a dominant $LQ\bar{D}$ coupling. The flavours of the decay products of the neutralino depend on the flavour structure of the Yukawa couplings λ_{ijk} and λ'_{ijk} . Heavier neutralinos can also decay *indirectly* to the lightest neutralino: $\chi' \rightarrow Z^*\chi$. The possible topologies arising from the pair-production of neutralinos ($\chi\chi$ and $\chi'\chi$) for a dominant $LL\bar{E}$ coupling are therefore: four to six leptons plus missing energy (\cancel{E}), and multi-leptons and hadrons plus \cancel{E} .

The chargino can decay *indirectly* to the neutralino: $\chi^+ \rightarrow W^*\chi$. The chargino can also decay *directly* to SM particles: $\chi^+ \rightarrow l^+l^-l^+$ or $\chi^+ \rightarrow \nu\nu l^+$ for $LL\bar{E}$. This typically happens when the sleptons/sneutrinos are lighter than the chargino, or when the chargino is the LSP. We assume the gauge unification condition [1]:

$$M_1 = \frac{5}{3} \tan^2 \theta_W M_2. \quad (2)$$

Under this assumption the chargino cannot be the LSP⁴, but we note that our analyses cover chargino LSP topologies. Summarising, the possible chargino topologies for a dominant $LL\bar{E}$ coupling are: six leptons, four to six leptons plus missing energy (\cancel{E}), acoplanar leptons (of same or mixed flavour), and multi-leptons and hadrons plus \cancel{E} . For a dominant $LQ\bar{D}$ coupling the indirect decay topologies are: multi-jet and multi-lepton and/or multi-neutrino states.

Sleptons and sneutrinos can decay *indirectly* to the lightest neutralino: $\tilde{l} \rightarrow l\chi$ and $\tilde{\nu} \rightarrow \nu\chi$. If the sleptons or sneutrinos are the LSPs, sleptons will dominantly decay *directly* to acoplanar leptons of same or mixed flavours, and sneutrinos to four lepton final states via a dominant $LL\bar{E}$ coupling. Ignoring mass mixing, only left-handed sleptons/sneutrinos can decay *directly* to four quarks via a dominant $LQ\bar{D}$ coupling.

Finally, stops and sbottoms can decay *indirectly* to the lightest neutralino for a dominant $LL\bar{E}$ coupling: $\tilde{t} \rightarrow c\chi$, and $\tilde{b} \rightarrow b\chi$. They cannot decay *directly* to SM particles via the purely leptonic $LL\bar{E}$ coupling. They can decay *directly* via the $LQ\bar{D}$ coupling and produce acoplanar jets or dileptons plus dijets, but these topologies are not considered in this paper.

In the following Section we describe the search analyses which cover the topologies outlined above.

3 Selection Criteria

The signal topologies for the direct and indirect decays were simulated using the SUSYGEN Monte Carlo (MC) program [16], and the MC samples were subsequently passed through the ALEPH detector simulation. Selection efficiencies were determined as a function of the SUSY particle masses, the generation structure of the R-parity violating coupling λ_{ijk} and λ'_{ijk} , the branching ratios of the indirect decays into SM particles and lighter SUSY states, and the branching ratios of the direct decays into all possible SM topologies. The selections presented below were optimised using the \bar{N}^{95} method advocated in [14], i.e. the cuts were tuned to give the optimal *expected* 95% C.L. excluded cross section using the signal efficiencies and the background estimates from Monte Carlo. Generally the selection efficiencies for the SUSY signals are high, typically in the range 50 – 90% for final states which contain a maximum number of electrons or muons (the “best case” scenarios), and

⁴At least for chargino masses $M_{\chi^+} > 45 \text{ GeV}/c^2$, which are not already excluded by LEP 1.

Coupling	Selection	SUSY signal	Background	Data
$LL\bar{E}$	Six Leptons	χ^+	0.1	0
	Six Leptons plus \cancel{E}	\tilde{l}, χ^+	0.1	0
	Four Leptons	$\tilde{\nu}$	0.8	0
	Four Leptons plus \cancel{E}	$\tilde{l}, \tilde{\nu}, \chi$	0.4	1
	Acoplanar Leptons	\tilde{l}, χ^+	12 ^(*)	15
	Leptons and Hadrons	χ^+, χ	0.8	1
$LQ\bar{D}$	Multi-jets plus Leptons and/or \cancel{E}	χ^+	2	3
	Four Jets	$\tilde{l}, \tilde{\nu}$	19 ^(**)	14 ^(**)

Table 2: *Selections, the SUSY signals which give rise to the above topologies, the number of expected background events, and the number of candidate events selected in the data ($\sqrt{s} = 130 - 172$ GeV). The value marked (*) is subtractable background. For (**) the total background/number of candidate events is quoted. Limits on the four jet topologies are then calculated using a sliding reconstructed di-jet mass window (Section 3.2.2), subtracting the expected background.*

30 – 50% for final states which contain a maximum number of taus (the “worst case” scenarios).

3.1 Topologies arising from the $LL\bar{E}$ couplings

The selections for a dominant $LL\bar{E}$ operator share one common property: they select topologies with multi-leptonic final states. The topologies can consist of as little as two acoplanar leptons in the simplest case, or they may consist of as many as six leptons plus two neutrinos in the more complicated case. In addition to the purely leptonic topologies, the MSSM cascade decays of heavier gauginos into lighter gaugino states may produce multi-jet and multi-lepton final states. We now describe the selections of the various topologies in turn. A brief summary of all selections, the expected number of background events from SM processes, and the number of candidates selected in the data is shown in Table 2.

3.1.1 Six Leptons

Six lepton topologies are expected from the cascade decays of charginos to lighter sneutrinos, which subsequently decay to leptons: $\chi^+ \rightarrow l^+ \tilde{\nu} \rightarrow l^+ l^+ l^-$. To select this topology the analysis requires at least five charged tracks (N_{ch}), but no more than 9, and at least four identified leptons (i.e. electrons or muons). The charged tracks should also be well separated, and therefore the Durham scale⁵ $y_3 > 0.01$ and $y_4 > 0.002$. No candidate was selected in the data at $\sqrt{s} = 130 - 172$ GeV.

3.1.2 Six Leptons plus Missing Energy

This topology is expected from the indirect decays of charginos and sleptons: $\chi^+ \rightarrow l^+ \nu \chi \rightarrow l^+ \nu l^+ l^- \nu$ and $\tilde{l}^+ \rightarrow l^+ \chi \rightarrow l^+ l^+ l^- \nu$. The selection requires at least five, but no more than

⁵The variable y_n is the maximum value of y_{Durham} at which the event is still reconstructed as a n-jet event using the Durham jet-finding algorithm [15].

eleven charged tracks, a visible mass (M_{vis}) between $25 \text{ GeV}/c^2$ and $85\%\sqrt{s}$, a missing p_T greater than $2\%\sqrt{s}$, and at least two identified leptons (N_{lep}). The remaining $q\bar{q}$ and $\tau^+\tau^-$ background is reduced by requiring y_4 to be greater than 0.004, and that the total charged energy be greater than 6 times the neutral hadronic energy. No candidate was found in the data.

3.1.3 Four Leptons

The topology is expected from the direct decays of sneutrinos: $\tilde{\nu} \rightarrow l^+l^-$. The preselection requires between four and six charged tracks, $M_{\text{vis}} > 30 \text{ GeV}/c^2$, and $y_3 > 0.007$ and $y_4 > 0.0004$. The selection is then split into three subselections for final states with no taus (requiring $N_{\text{lep}} \geq 3$, a total momentum along the beam axis less than 25 GeV , and a neutral hadronic energy less than 15% of the leptonic energy), with two taus (requiring two identified leptons of same flavour, missing $p_T > 2\%\sqrt{s}$ and a neutral hadronic energy less than 30% of the leptonic energy), and with four taus (no energy within 12° of the beam pipe and a neutral hadronic energy less than 30% of the leptonic energy). The three subselections are finally ORed. No candidate was selected in the data.

3.1.4 Four Leptons plus Missing Energy

The topology arises from the pair production of the lightest neutralino $\chi\chi \rightarrow lll\nu\nu$, from associated neutralino production where the $Z^* \rightarrow \nu\bar{\nu}$, from the indirect decays of sneutrinos $\tilde{\nu} \rightarrow \nu\chi$, from the ‘‘mixed’’ decays of sleptons, where one slepton decays directly, and the other decays indirectly, and the direct decays of charginos ($\chi^+\chi^- \rightarrow (l^+\nu\nu)(l^+l^-)$). The selection requires between four and six charged tracks, $M_{\text{vis}} > 16 \text{ GeV}/c^2$, at least one identified lepton, total missing $p_T > 5 \text{ GeV}$ and $y_4 > 0.0006$. Finally jets are built using the JADE algorithm with a value of $y_{\text{cut}} > (M_\tau^2/s)$ such that jets of the tau mass are formed. At least four of the jets are required to contain charged tracks. The total expected background of 0.4 events is dominated by four fermion processes. One candidate is selected in the data at $\sqrt{s} = 172 \text{ GeV}$, which is consistent with the $e^+e^- \rightarrow \gamma^*Z \rightarrow e^+e^-\tau^+\tau^-$ process.

3.1.5 Acoplanar Leptons

Right-handed sleptons of flavour k can decay into leptons of flavour i or j and neutrinos via the coupling λ_{ijk} , producing acoplanar lepton topologies of same or mixed flavours. Similarly charginos can decay to a slepton and a sneutrino, which subsequently decay to a lepton and a neutrino: $\chi^+ \rightarrow \nu\tilde{l}^+ \rightarrow \nu l^+\nu$. Selections for the topology of two acoplanar leptons of same flavour have already been developed for the search for sleptons under the assumption that R-parity is conserved [17], and are here extended to allow for mixed lepton flavours. The total expected background of 12 events is irreducible, coming nearly entirely from the leptonic decays of W pairs, and we therefore subtract this background according to the prescription given in [19] to derive upper limits on the production cross sections. A total of 15 events are selected in the data, consistent with the SM expectation. Table 3 shows the number of candidates selected in the various topologies. These events display clear characteristics of leptonic WW decays.

Topology	ee	$\mu\mu$	$\tau\tau$	$e\mu$	$e\tau$	$\mu\tau$
Selected in Data	1	1	1	4	3	5

Table 3: *The number of candidate events selected in the data by the acoplanar lepton selection, listed according to lepton flavours.*

3.1.6 Leptons and Hadrons

This topology is expected from the indirect decays of charginos and the heavier neutralinos to the lightest neutralino: $\chi^+ \rightarrow W^*\chi \rightarrow W^*l^+l^-\nu$ and $\chi' \rightarrow Z^*\chi \rightarrow Z^*l^+l^-\nu$, where at least one W^* or Z^* decays hadronically. Three subselections have been designed to guarantee good efficiencies independent of the phase space available for the W^* and Z^* : a selection for low multiplicity, for high multiplicity and for small leptonic energy. The low multiplicity selection selects events with less than 16 charged tracks, $20 \text{ GeV}/c^2 < M_{\text{vis}} < 75\%\sqrt{s}$, total missing $p_T > 2.5\sqrt{s}$, small hadronic energy (E_{had}) and large leptonic energy (E_{leptons}), which cluster at $y_3 > 0.009$ and $y_4 > 0.0026$ into three and four jets, respectively. The high multiplicity selection requires more than four charged tracks, $M_{\text{vis}} > 25$, the total transverse and longitudinal momenta $p_T > 3.5\%\sqrt{s}$ and $p_z < 27 \text{ GeV}$, large leptonic energy, and $y_5 > 0.006$. The small leptonic energy selection requires more than nine charged tracks, a visible mass in the window $55\%\sqrt{s} < M_{\text{vis}} < 80\%\sqrt{s}$, a leptonic energy in excess of $20\%E_{\text{had}}$, total missing $p_T > 5\sqrt{s}$, a thrust less than 0.85, large y_3, y_4, y_5 values, and no isolated photon jets (i.e. jets with dominantly electromagnetic energy, and no charged track) to be found in the event. Finally, the three subselections are ORed, and a veto against the WW background is applied using the hadronic mass $m_{q\bar{q}}$, the momentum of the highest energy lepton, and the invariant mass of the lepton/missing energy system $m_{l\nu}$. The total expected background is 0.8 events, mainly from $q\bar{q}$ and W-pair-production. One event is selected in the data, consistent with a $WW \rightarrow q\bar{q}e\nu$ event.

3.2 Topologies arising from the $LQ\bar{D}$ couplings

For a dominant $LQ\bar{D}$ operator the event topologies are mainly characterised by large hadronic activity, possibly with some leptons and/or missing energy. In the simplest case the topology consists of four jet final states, and in the more complicated scenario of multi-jet and multi-lepton and/or multi-neutrino states.

3.2.1 Multi-jets plus Leptons and/or missing Energy

This topology is expected from the indirect decays of charginos to neutralinos: $\chi^+ \rightarrow W^*\chi \rightarrow W^*lqq$ or $\chi^+ \rightarrow W^*\nu qq$. Depending on the W^* phase space and decay mode, the topology may resemble a purely hadronic final state, a leptonic final state with some hadronic activity, or a mix thereof. After a common preselection, requiring $N_{\text{ch}} \geq 10$, $M_{\text{vis}} > 45$, and the polar angle of the missing energy vector $\theta_{\text{miss}} > 30^\circ$, three subselections have been designed to address the different cases. In the following primed event variables denote quantities which are calculated excluding identified leptons. This procedure ensures equal treatment of leptons and neutrinos (i.e. missing energy) from the neutralino decays $\chi \rightarrow l^\pm qq'$ and $\chi \rightarrow \nu qq'$.

The hadronic subselection requires the visible mass $M'_{\text{vis}} > 43\%\sqrt{s}$, that the energy deposited in the calorimeter around a narrow cone along the direction of the missing energy

vector $E_{\text{miss}}^{\text{isolated}} < 5 \text{ GeV}$, a thrust less than 0.9, $(y_5, y_6) > (0.003, 0.002)$, that all jets contain less than 90% electromagnetic energy, and transverse energy $E_T < 60 \text{ GeV}$. Finally a two-dimensional cut is applied in the $(M'_{\text{vis}}, \phi'_{\text{acoplanarity}})$ plane. The leptonic subselection requires $M'_{\text{vis}} < 65\% \sqrt{s}$, $\text{thrust} < 0.8$, $y'_4 > 0.001$, $y_6 > 0.00035$, and $E_{\text{had}} < 47\% E_{\text{leptons}}$, $E_{\text{leptons}} < 40 \text{ GeV}$, and a WW veto similar to the one described in Section 3.1.6. The mixed subselection requires $M'_{\text{vis}} < 50\% \sqrt{s}$, $\text{thrust} < 0.74$, $y'_4 > 0.0047$, $E_{\text{had}} < 2.5 E_{\text{leptons}}$, a two-dimensional cut in the $(y_6, \phi'_{\text{acoplanarity}}^{\text{projected}})$ plane, $E_{\text{leptons}} < 40 \text{ GeV}$, and a WW veto. Finally the three subselections are ORed. The total expected background is 2 events, dominated by WW and $q\bar{q}$ processes. Three events are selected in the data. Two of the three events are consistent with a $q\bar{q}$ interpretation. The third event displays characteristics of a $W e \nu \rightarrow q \bar{q} e \nu$ event.

3.2.2 Four Jet final states

Sleptons and sneutrinos can decay directly into four jet final states. Normally one considers the pair production of equal mass sleptons, as for example in the pair production of left-handed sleptons: $\tilde{l}_L^+ \tilde{l}_L^- \rightarrow q_1 \bar{q}_2 q_3 \bar{q}_4$. The four jet system will then also have the property that the invariant di-jet masses are equal: $M_{\text{inv}}(q_1, q_2) = M_{\text{inv}}(q_3, q_4)$. In this section we use an analysis which was originally developed for the search for charged Higgses decaying into charm and strange quarks [18].

After requiring at least 8 charged particle tracks and a total charged energy of more than $10\% \sqrt{s}$, events from $q\bar{q}(\gamma)$ are rejected by a two-dimensional cut in p_{miss}^z and M_{vis} . Spherical events with thrust less than 0.9 are then clustered into four jets and kept if $y_4 > 0.006$. After vetoing events with photon-like jets, events that match the equal dijet mass hypothesis are selected by cutting on the mass difference of the dijet systems, and by performing a 5C-fit (energy-momentum conservation and equal mass constraint) that is required to lead to a small χ^2 . Within a window of $M_{5C} \pm 3 \text{ GeV}/c^2$, efficiencies are of the order of 35%, and a total background of 18.7 events is expected at $\sqrt{s} = 130 - 172 \text{ GeV}$ for $M_{5C} < 70 \text{ GeV}/c^2$. In agreement with this expectation, 14 events are observed in the data, with a dijet mass distribution in agreement with the Standard Model prediction, as is shown in Fig. 1. Limits on slepton and sneutrino production are set by sliding a mass window across this distribution, counting the number of events seen and subtracting the expected background, conservatively reducing the expected background by 20%.

4 Limits on Sparticles for a dominant $LL\bar{E}$ coupling

None of the above analyses find evidence for Supersymmetry in the data collected at $\sqrt{s} = 130 - 172 \text{ GeV}$. In this section we interpret the negative results of the search analyses in terms of limits on the masses of the SUSY particles.

4.1 Charginos and Neutralinos

Charginos and neutralinos can decay either *indirectly* via the lightest neutralino, or *directly* via sleptons or sneutrinos. The corresponding branching fractions in general depend on the field content and masses of the charginos and neutralinos, the sfermion mass spectrum as well as the Yukawa coupling λ . For simplicity, this analysis considers the two extreme cases of either indirect or direct decays only, not addressing the region of parameter space

where both decays have sizable branching fractions. Limits have been evaluated assuming a common slepton and sneutrino mass m_0 at the GUT scale, which according to the renormalisation group equations [20] links the selectron and electron-sneutrino masses at the EW scale by

$$\begin{aligned} m_{\tilde{e}_R}^2 &= m_0^2 + 0.22 M_2^2 - \sin^2\theta_W M_Z^2 \cos 2\beta \\ m_{\tilde{e}_L}^2 &= m_0^2 + 0.75 M_2^2 - \frac{1}{2}(1 - 2\sin^2\theta_W)M_Z^2 \cos 2\beta \\ m_{\tilde{\nu}_e}^2 &= m_0^2 + 0.75 M_2^2 + \frac{1}{2}M_Z^2 \cos 2\beta \end{aligned}$$

The calculated masses $m_{\tilde{e}}, m_{\tilde{\nu}_e}$ are only used in the computation of the neutralino (chargino) cross section, which receives a positive (negative) contribution due to t-channel selectron (sneutrino) exchange, respectively.

4.1.1 Dominance of indirect decays

In this scenario all charginos and neutralinos are assumed to decay to the lightest neutralino, which then decays violating R-parity into two charged leptons and a neutrino. For charginos the ‘‘Leptons and Hadrons’’ selection is ORed with the ‘‘Six Leptons plus Missing Energy’’ selection, and for neutralinos ($\chi\chi$) and ($\chi'\chi$) the logical OR of the ‘‘Leptons and Hadrons’’ and the ‘‘Four and Six Leptons plus Missing Energy’’ analyses are used to determine the signal efficiencies as a function of $M_{\chi^+}, M_{\chi'}, M_{\chi}$ ⁶ and the choice of generation indices i, j, k of the coupling λ_{ijk} . For a given value of m_0 and $\tan\beta$, limits are derived in the (μ, M_2) plane for the worst case in terms of generation indices i, j, k and squark masses⁷. In most points this worst case is identified as a dominant 133-coupling⁸ and small squark masses, leading to a large hadronic branching fraction with low selection efficiency. The limits set this way are by construction independent of the choice of generation indices or squark masses.

In each point for a fixed $\mu - M_2 - m_0 - \tan\beta$, the \bar{N}_{95} -prescription is applied to decide whether to combine chargino and neutralino searches to obtain the best exclusion power. Fig. 2 shows the limits obtained in the (μ, M_2) plane for a fixed value of $\tan\beta$ and m_0 . Scanning $\tan\beta$ and m_0 , the limits are translated into limits on the mass of the lightest chargino and neutralino, which are shown as a function of $\tan\beta$ in Fig. 3. Since the worst case limit is basically set by the purely hadronic decays, the $\tan\beta$ -dependence of the two mass limits is dictated mainly by the relative change of the chargino and neutralino mass isolines in the (μ, M_2) plane with respect to $\tan\beta$. At values of $\tan\beta$ close to one, small neutralino masses are excluded by an interplay of limits on $\chi\chi'$ -production from LEP1 and the LEP2 chargino and neutralino limits (see Fig. 4), in the case of $\tan\beta = 1$ still allowing neutralino masses as small as 25 GeV.

⁶Efficiencies are parameterised down to neutralino masses of $M_{\chi} = 10 \text{ GeV}/c^2$. For $M_{\chi} \lesssim 10 \text{ GeV}/c^2$ the neutralino lifetime can exceed a mean free path of flight of 1cm, and therefore fall outside our assumption of negligible lifetime. For this reason points with $M_{\chi} < 10 \text{ GeV}/c^2$ in SUSY parameters space are not considered.

⁷Varying the squark mass corresponds to changing the leptonic to hadronic branching ratios of the chargino (and neutralino) decays $\chi^+ \rightarrow l^+ \nu_{\chi}, qq'\chi$.

⁸The coupling λ_{133} corresponds to a maximum number of taus in the final state, which generally leads to worst case detection efficiencies. The coupling λ_{122} corresponds to a maximum number of muons in the final state, the best case scenario.

4.1.2 Dominance of direct decays

Assuming the widths for the decays via the lightest neutralino to be negligible relative to the direct decays, charginos can decay either into one charged lepton plus two neutrinos or into three charged leptons, leading to two-, four- or six-lepton topologies. The composition of lepton flavours appearing in these final states depends on the field content of the chargino, the generation indices and the details of the mass spectrum. For simplicity, a logical OR of all corresponding selections is used. All branching fractions and flavour compositions have been scanned to identify the overall most conservative efficiency (found for $\tau\tau$ final states), which is used to set limits valid for all choices of these parameters.

For the scenario considered here all neutralinos are assumed to decay to two charged leptons plus a neutrino. Using the “Four Leptons plus missing Energy” selection, efficiencies have been calculated as a function of the neutralino masses for each possible flavour composition in the final state. As before, the smallest efficiency - corresponding to a maximum number of taus in the final state - is used to set limits independent of the choice of generation indices.

In analogy to the procedure described in the previous section, limits from chargino and neutralino searches are set for each point in $\mu - M_2 - \tan\beta - m_0$ parameter space. Fig. 5 shows an example of the limit obtained in the gaugino region at $m_0 = 60 \text{ GeV}/c^2$. Due to the destructive interference of the s - and t -channel contributions to the chargino cross section, the limit set by the chargino search does not reach the kinematic limit at small m_0 . On the other hand, the production cross section for $\chi\chi$ is enhanced at small selectron masses, allowing to exclude charginos well beyond the kinematic limit in certain regions of parameter space.

After scanning the parameter space in $\mu - M_2 - m_0$, the information is summarised in terms of limits on the masses of the lightest chargino and neutralino as a function of $\tan\beta$ as shown in Fig. 3. The limits, $M_{\chi^+} > 73 \text{ GeV}/c^2$ and $M_\chi > 23 \text{ GeV}/c^2$, hold for any choice of generation indices i, j, k , and for neutralino, slepton and sneutrino LSPs.

4.2 Sleptons

Sleptons can decay either directly to a lepton and a neutrino, producing acoplanar lepton topologies of same or mixed flavour, or indirectly to a lepton and a neutralino⁹ (which subsequently decays to two leptons and a neutrino) producing six lepton plus two neutrino topologies. For the indirect decays a logical OR of the “Six Leptons plus Missing Energy” and “Four Leptons plus Missing Energy” selection is used to determine the excluded cross section as a function of $M_{\tilde{l}}$, M_χ and the generation indices i, j, k . Generally, the couplings λ_{122} and λ_{133} correspond to the best and worst case exclusion, producing topologies with a maximum number of muons and taus, respectively. For the direct decays the “Acoplanar Lepton” analysis is used to set the limit. Although efficiencies for the acoplanar lepton topologies are high, the large expected background in this channel (which is subtracted) leads to an exclusion limit which is worse than the limit for the indirect decays. The limits on the mass of the right-handed sleptons are shown in Fig. 6. The slepton mass limits for the indirect decay modes, the most conservative choice of coupling (λ_{133}), and for $M_\chi > 23 \text{ GeV}/c^2$ (the neutralino limit derived in Section 4.1), are: $M_{\tilde{e}_R} > 63 \text{ GeV}/c^2$

⁹The decays to charginos (the chargino limit is $M_{\chi^+} > 78 \text{ GeV}/c^2$, from the previous Section) are kinematically inaccessible for most of the slepton mass range considered in this Section.

(gaugino region, $\mu = -200 \text{ GeV}/c^2$, $\tan \beta = \sqrt{2}$), $M_{\tilde{\mu}_R} > 62 \text{ GeV}/c^2$, $M_{\tilde{\tau}_R} > 56 \text{ GeV}/c^2$.

4.3 Sneutrinos

Sneutrinos can decay either directly into pairs of charged leptons, or indirectly to a neutrino and a neutralino, which subsequently decays to two leptons and a neutrino. The “Four Lepton” selection for the direct decays, and the “Four Leptons plus \cancel{E} ” selection for the indirect decays is employed to set limits on the sneutrino cross section as a function of $M_{\tilde{\nu}}$, M_χ , and the generation indices i, j, k . As for the sleptons, the best case and worst case for the indirect decays correspond to the couplings λ_{122} and λ_{133} , respectively. The limits are shown in Fig. 7. The sneutrino mass limits for the indirect decay modes, the most conservative choice of coupling (λ_{133}), and for $M_\chi > 23 \text{ GeV}/c^2$ are: $M_{\tilde{\nu}_e} > 72 \text{ GeV}/c^2$ (gaugino region, $\mu = -200 \text{ GeV}/c^2$, $\tan \beta = \sqrt{2}$), $M_{\tilde{\nu}_\mu}, M_{\tilde{\nu}_\tau} > 49 \text{ GeV}/c^2$.

4.4 Squarks

Stops and sbottoms can only decay indirectly to neutralinos for a dominant $LL\bar{E}$ coupling: $\tilde{t} \rightarrow c\chi$, and $\tilde{b} \rightarrow b\chi$, with the neutralino decaying subsequently into two charged leptons and a neutrino. The “Leptons and Hadrons” selection is used to derive limits on the stop and sbottom masses, which are shown in Fig. 8. The most conservative limits, corresponding to the coupling λ_{133} , are: $M_{\tilde{t}_L} > 60 \text{ GeV}/c^2$ and $M_{\tilde{b}_L} > 58 \text{ GeV}/c^2$ for $M_\chi > 23 \text{ GeV}/c^2$.

5 Limits on Sparticles for a dominant $LQ\bar{D}$ coupling

5.1 Chargino limits

The indirect decays of the chargino to the neutralino produce multi-jets plus leptons and/or missing energy. The efficiencies for these topologies are determined as a function of M_{χ^+} , M_χ and the generation indices i, j, k of the coupling λ'_{ijk} using the “Multi-jets plus Leptons and/or missing Energy” selection. This selection has lowest efficiencies for final states with taus, which corresponds to the worst case coupling λ_{3jk} . The chargino limits are derived in the same way as for the $LL\bar{E}$ operator, i.e. for the choice of generation indices i, j, k and squark masses which give the most conservative exclusion. Since the analysis only covers the indirect decay topologies at present, the limits are derived for large m_0 , and assuming that the stop and sbottoms are heavier than the chargino. The excluded regions in the (M_2, μ) plane are shown in Fig. 9. Charginos are excluded at the 95% C.L. nearly to the kinematic limit. $M_{\chi^+} > 83, 85 \text{ GeV}/c^2$ for $\tan \beta = \sqrt{2}, 35$, respectively, and $m_0 = 500 \text{ GeV}/c^2$.

5.2 Slepton and Sneutrino Limits

Sleptons and sneutrinos can decay directly to four jet final states via the $LQ\bar{D}$ coupling. The “Four Jet” analysis is used to set an upper limit on the production cross section of left-handed sleptons¹⁰ and sneutrinos. The cross section limit is shown as a function of the slepton/sneutrino mass in Fig. 10. The corresponding mass limits are: $M(\tilde{e}_L) > 51 \text{ GeV}/c^2$

¹⁰Neglecting mixing effects in the slepton sector, only left-handed sleptons can decay directly to SM particles via the $LQ\bar{D}$ couplings.

evaluated at a point in the deep higgsino region ($\mu = -100 \text{ GeV}/c^2$, $M_2 = 1 \text{ TeV}/c^2$, $\tan \beta = \sqrt{2}$) and assuming the gauge unification condition Eq.(2)); and $M(\tilde{\mu}_L, \tilde{\tau}_L) > 51 \text{ GeV}/c^2$, $M(\tilde{\nu}) > 51 \text{ GeV}/c^2$. The limits assume that the sleptons and sneutrinos decay directly to four jets with a branching ratio of unity.

6 Implications for the High Q^2 HERA Events and the ALEPH four jet Anomaly

The recently reported excess of high Q^2 events at HERA [9] may be interpreted [8] as a s-channel squark resonance in R-parity violating models, where the produced squark of mass $M_{\tilde{q}} \sim 200 \text{ GeV}/c^2$ decays via a dominant $LQ\bar{D}$ coupling to a positron and a quark. As discussed in the literature, a number of coupling solutions exist which are consistent with low energy bounds on λ' and can explain the HERA excess at the same time. Since limits from the Tevatron [21] exclude $M_{\tilde{q}} \leq 210 \text{ GeV}/c^2$ if the branching ratio $B(\tilde{q} \rightarrow e^+q) = 1$, additional squark decay modes to lighter charginos or neutralinos are expected, possibly within the reach of LEP 2. The negative result of the chargino search constrains the allowed regions in SUSY parameter space to $M_{\chi^+} > 83 \text{ GeV}/c^2$ (for $\tan \beta = \sqrt{2}$). Fig. 11 shows contours of varying branching ratios $B(\tilde{q} \rightarrow e^+q)$ in the (μ, M_2) plane for the solution $\tilde{c}_L \rightarrow e^+d$, $\lambda_{121} = 0.04$, with the ALEPH chargino limit superimposed. The limit constrains interesting regions for the HERA interpretation in the deep higgsino region ($M_2 \gtrsim 550 \text{ GeV}/c^2$), where the chargino coupling to the scalar charm is small compared to the R-parity violating Yukawa coupling $\lambda_{121} = 0.04$.

ALEPH has previously reported an anomaly in four jet events [23] recorded at centre-of-mass energies between 130 and 172 GeV, for which the observed distribution of the sum of the two dijet invariant masses constructed by pairing jets with the smallest dijet mass difference shows a peak around $\sim 106 \text{ GeV}/c^2$, with a small dijet mass difference. In [10] the anomaly was interpreted as selectron pair-production $\tilde{e}_L\tilde{e}_R$ (with $M_{\tilde{e}_L} - M_{\tilde{e}_R} \sim 10 \text{ GeV}/c^2$), where the selectrons subsequently decay directly via $LQ\bar{D}$ to four jet final states. In this model the production cross section $\sigma(\tilde{e}_L\tilde{e}_R)$ can be much larger than $\sigma(\tilde{e}_R\tilde{e}_R, \tilde{e}_L\tilde{e}_L)$, as illustrated in Fig. 12. Since the equal mass four jet analysis finds good agreement between data and SM expectation, the model is now constrained by the cross section limit on $\tilde{e}_R\tilde{e}_R$ derived¹¹ in Section 3.2.2: for $\sigma_{\text{ex}} = 0.55 \text{ pb}$ (at $M_{\tilde{e}} = 48 \text{ GeV}/c^2$), the U(1) gaugino parameter is constrained to $M_1 > 68 \text{ GeV}/c^2$ in Fig. 12.

7 Conclusions

The searches for R-parity violating SUSY topologies find no evidence for Supersymmetry in the data collected at $\sqrt{s} = 130 - 172 \text{ GeV}$. The negative results translate into the following mass limits for a dominant $LL\bar{E}$ coupling at the 95% C.L.: for the gauginos $M_{\chi^+} > 73 \text{ GeV}/c^2$, $M_{\chi} > 23 \text{ GeV}/c^2$, valid for any choice of coupling, and valid for neutralino, slepton or sneutrino LSPs. For the scalar fermions (indirect decay modes): $M_{\tilde{e}_R} > 63 \text{ GeV}/c^2$ (gaugino region), $M_{\tilde{\mu}_R} > 62 \text{ GeV}/c^2$, $M_{\tilde{\tau}_R} > 56 \text{ GeV}/c^2$, $M_{\tilde{t}_L} > 60 \text{ GeV}/c^2$, $M_{\tilde{b}_L} > 58 \text{ GeV}/c^2$, again valid for any choice of coupling.

¹¹For non-negligible mixing in the slepton sector (assumed in [10]), left- and right-handed selectrons can decay directly via the $LQ\bar{D}$ operator.

For a dominant $LQ\bar{D}$ coupling, chargino masses are excluded nearly up to the kinematic limit: $M_{\chi^+} > 83 \text{ GeV}/c^2$ for $\tan\beta = \sqrt{2}$ and $m_0 = 500 \text{ GeV}/c^2$, valid for any choice of coupling. Assuming the dominance of direct decay modes of sleptons and sneutrinos to four jet final states, $M(\tilde{e}_L) > 51 \text{ GeV}/c^2$ (higgsino region), and $M(\tilde{\mu}_L, \tilde{\tau}_L), M(\tilde{\nu}) > 51 \text{ GeV}/c^2$.

The results for $LQ\bar{D}$ have implications for the R-parity violating interpretations of the high Q^2 events at HERA, and the ALEPH four jet anomaly. In both cases, the interesting regions of parameter space are constrained by the results presented in this paper.

8 Acknowledgements

It is a pleasure to congratulate our colleagues from the accelerator division for the successful operation of LEP above the W threshold. We would like to express our gratitude to the engineers and support people at our home institutes without whose dedicated help this work would not have been possible. Those of us from non-member states wish to thank CERN for its hospitality and support.

References

- [1] For a review see for example H.P. Nilles, Phys. Rep. 110 (1984) 1; H.E. Haber and G.L. Kane, Phys. Rept. 117 (1985) 75.
- [2] S. Weinberg, Phys. Rev. D 26 (1982) 287; N. Sakai and T. Yanagida Nucl. Phys. B 197 (1982) 83; S. Dimopoulos, S. Raby and F. Wilczek, Phys. Lett. B 212 (1982) 133.
- [3] L.J. Hall and M. Suzuki, Nucl. Phys. B 231 (1984) 419.
- [4] A. Chamseddine and H. Dreiner, Nucl. Phys. B 458 (1996) 65.
- [5] For example: D. E. Brahm, L. J. Hall, Phys. Rev. D 40 (1989) 2449, L. E. Ibanez, G. G. Ross, Nucl. Phys. B 368 (1992) 3; A. Yu. Smirnov, F. Vissani, Nucl. Phys. B 460 (1996) 37; A.H. Chamseddine, H. Dreiner, Nucl. Phys. B 447 (1995) 195.
- [6] The ALEPH Collaboration, Phys. Lett. B 349 (1995) 238.
- [7] The ALEPH Collaboration, Phys. Lett. B 384 (1996) 461.
- [8] D. Choudhury, and S. Raychaudhuri, Phys.Lett. B401 (1997) 54-61; G. Altarelli, J. Ellis, G. Giudice, S. Lola, and M. Mangano, CERN-TH-97-040, hep-ph/9703276; H. Dreiner and P. Morawitz, IC/HEP/97-2, hep-ph/9703279; J. Kalinowski, R. Ruckl, H. Spiesberger, P.M. Zerwas, Z.Phys. C 74 (1997) 595-603; T. Kon, T. Kobayashi, hep-ph/9704221; R. Barbieri, Z. Berezhiani, A. Strumia, hep-ph/9704275 ; A. S. Belyaev, A. V. Gladyshev, hep-ph/9704343; G. Altarelli, G. F. Giudice, M. L. Mangano, hep-ph/9705287; J. Ellis, S. Lola, K. Sridhar, hep-ph/9705416; J. Kalinowski, hep-ph/9706203; J. E. Kim, P. Ko, hep-ph/9706387; A. S. Joshipura, V. Ravindran, S. K. Vempati, hep-ph/9706482; S. Lola, hep-ph/9706519.
- [9] The H1 Collaboration, Z.Phys. C 74 (1997) 191; The ZEUS Collaboration, Z.Phys. C 74 (1997) 207.

- [10] M. Carena, G.F. Giudice, S. Lola, C.E.M. Wagner, Phys.Lett. B 395 (1997) 225.
- [11] H.P.Nilles, Phys.Rep. 110 (1984) 1; H.Haber and G.Kane, *ibid.* 117 (1985) 75; A.B.Lahanas and D.V.Nanopoulos, *ibid.* 145 (1987) 1.
- [12] J.Ellis, et al., Nucl.Phys. B 238 (1984) 453.
- [13] H. Dreiner and P.Morawitz, Nucl. Phys. B 428 (94) 31; H. Dreiner, S. Lola, P. Morawitz, Phys. Lett. B 389 (1996) 62.
- [14] The ALEPH Collaboration, Phys. Lett. B 384 (1996) 427.
- [15] Proceedings of the Durham Workshop, W.J.Stirling, J.Phys. G: Nucl. Part. Phys. 17 (1991) 1567; N. Brown and W.J.Stirling, Phys. Lett. B252 (1990) 657; S. Bethke, Z. Kunszt, D.E. Soper and W.J. Stirling, Nucl. Phys. B370 (1992) 310.
- [16] S. Katsanevas and M. Melachroinos, SUSYGEN, Proceedings of the Workshop *Physics at LEP 2*, eds. G. Altarelli, T. Sjöstrand, and F. Zwirner, CERN 96-01; and SUSYGEN V2, <http://lyohp5.in2p3.fr/delphi/katsan/susygen.html>.
- [17] The ALEPH Collaboration, CERN PPE/97-056, submitted to Physics Letters B.
- [18] The ALEPH Collaboration, "Search for charged Higgs-Bosons in e+e- collisions at centre-of-mass energies from 130 to 172 GeV", contribution to the 1997 EPS-HEP Conference, Jerusalem, Ref:613.
- [19] R.M. Barnett et al., Phys. Rev. D 54 (1996) 1.
- [20] K. Inoue, A. Kakuto, H. Komatsu, and S. Takeshita, Prog. Theor. Phys. 68 (1982) 927; *ibid.* 71 (1984) 413.
- [21] F. Abe et. al., CDF Collaboration, Phys. Rev. Lett. 77 (1996) 5336; C. Grosso-Pilcher, for the CDF Collaboration, talk at Vanderbilt Conference, "Frontiers in Contemporary Physics - Fundamental Particles and Interactions", May 1997.
- [22] G. Altarelli, J. Ellis, G. Giudice, S. Lola, and M. Mangano, CERN-TH-97-040, hep-ph/9703276.
- [23] The ALEPH Collaboration, Z.Phys. C 71 (1996) 179.

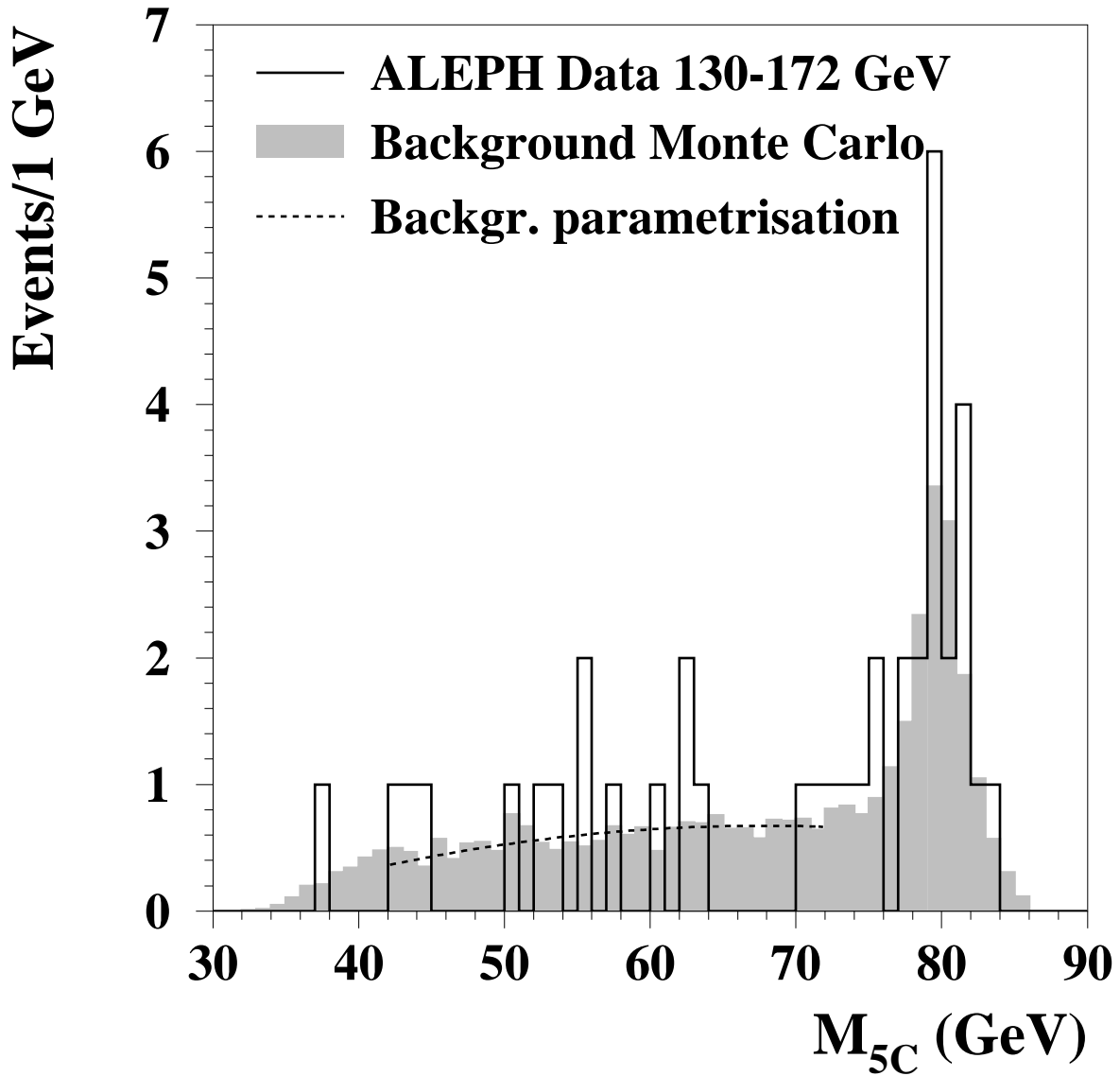


Figure 1: *The plot shows the expected reconstructed dijet-mass distribution of four jet final states after a 5C-fit equal mass constraint fit, and the distribution observed in the data. In the interesting region below the WW threshold, $M_{5C} < 70 \text{ GeV}/c^2$, a total number of 18.7 events are expected, in agreement with the observed 14 events. Also shown is the background parameterisation used for the background subtraction procedure.*

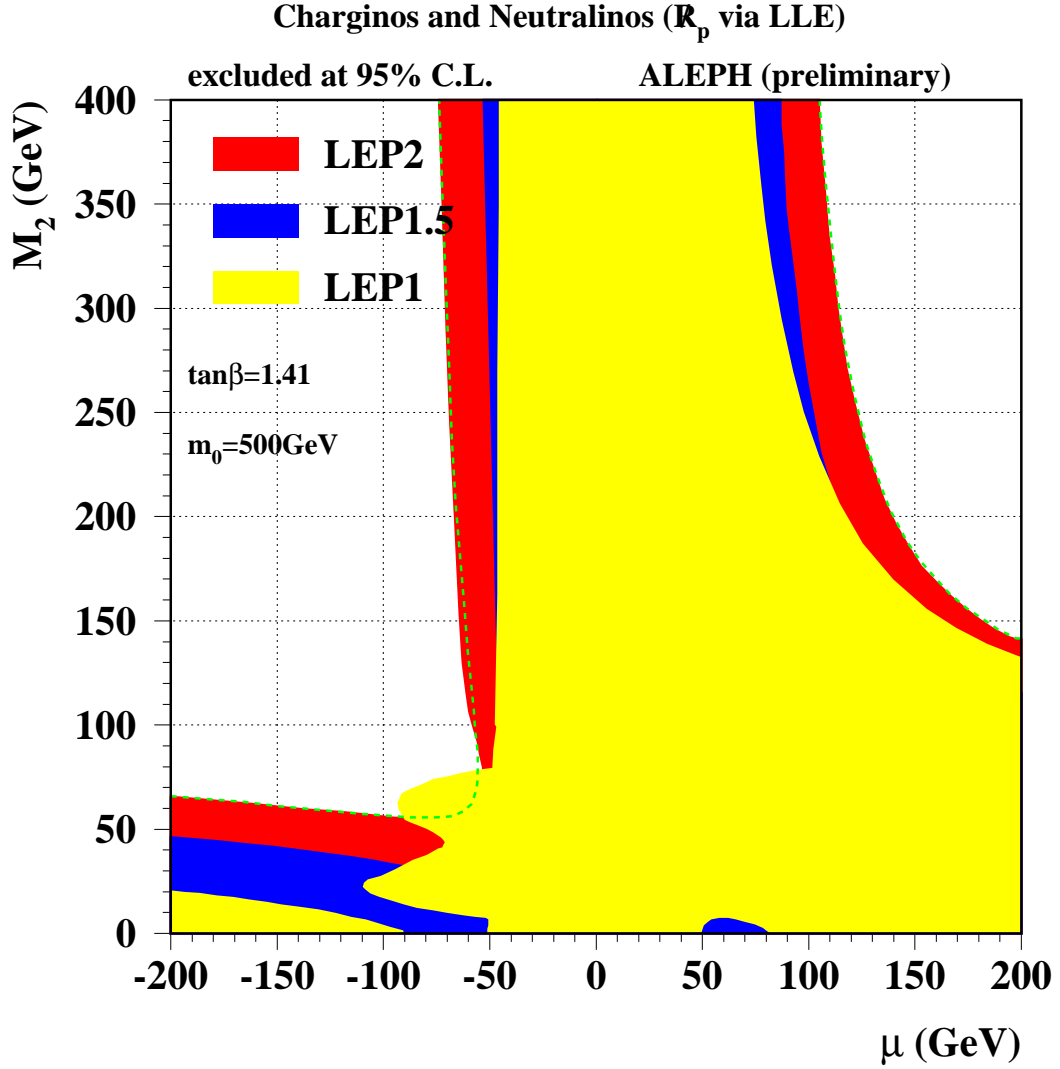


Figure 2: Regions in the (μ, M_2) plane excluded at the 95% C.L. for a dominant $LL\bar{E}$ coupling and fixed values of $\tan\beta = 1.41$ and $m_0 = 500 \text{ GeV}/c^2$, assuming that the indirect decays dominate. The superimposed dashed line shows the kinematic limit $M_{\chi^+} = 86 \text{ GeV}/c^2$.

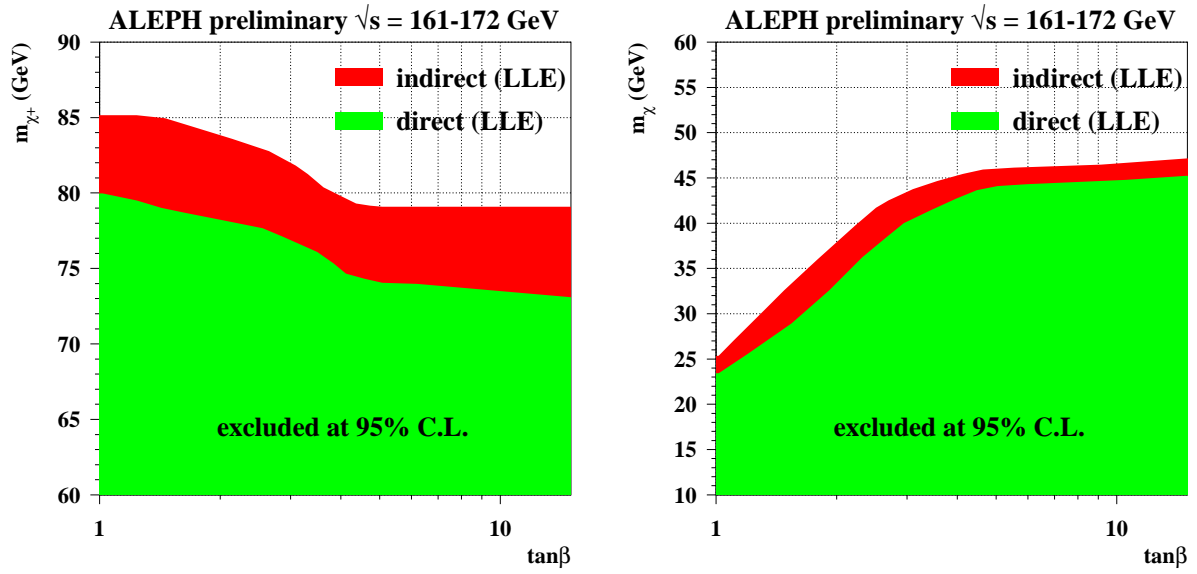


Figure 3: The 95% C.L. limit on the chargino mass (left) and the lightest neutralino mass (right) as a function of $\tan\beta$ for a dominant $L\bar{L}\bar{E}$ coupling, assuming the dominance of either direct or indirect decay modes. The limits hold for any choice of m_0 and the generation indices i, j, k of the coupling λ_{ijk} .

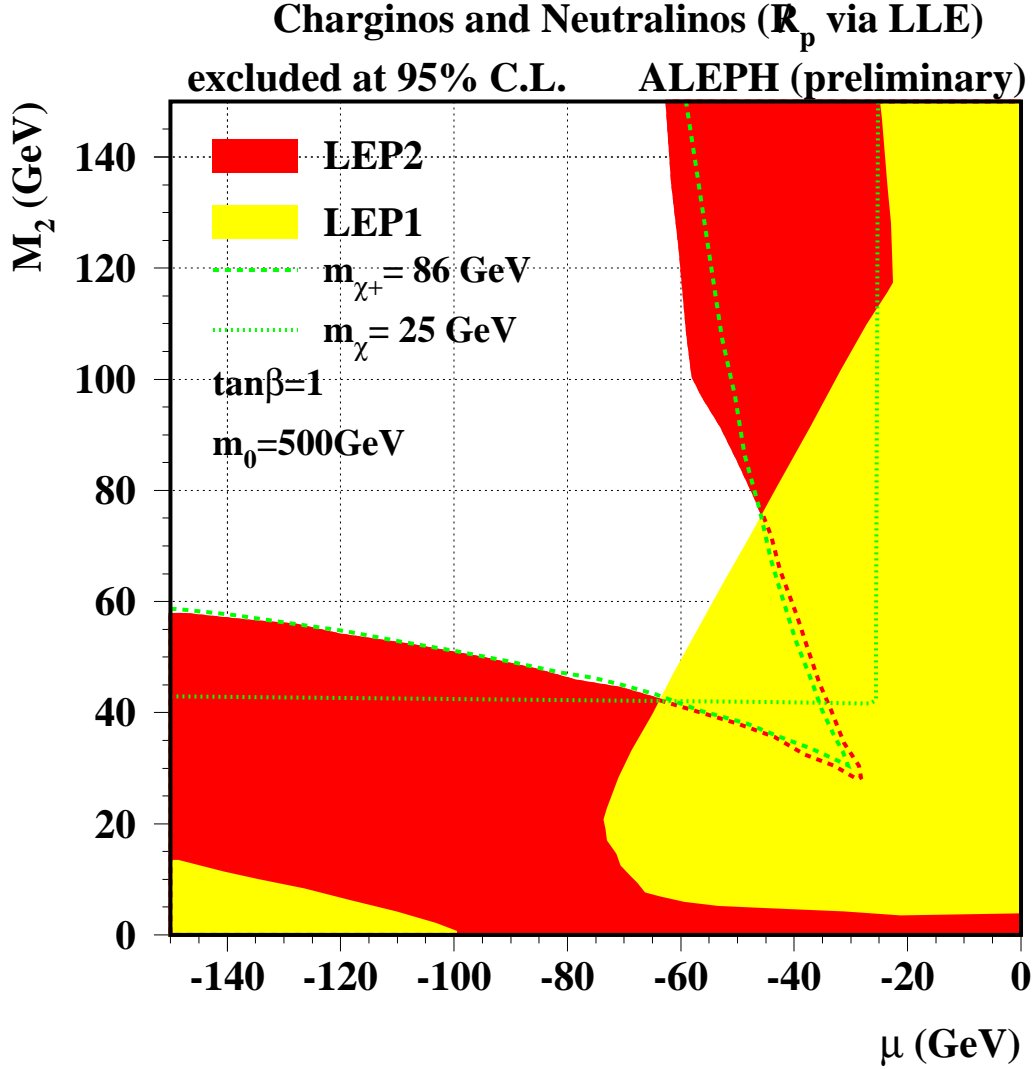


Figure 4: *Excluded regions at the 95% C.L. in the (μ, M_2) plane for a dominant $LL\bar{E}$ coupling and fixed values of $\tan\beta = 1$ and $m_0 = 500 \text{ GeV}/c^2$, assuming that the indirect decays dominate. The superimposed dashed and dotted lines show the kinematic limit $M_{\chi^+} = 86 \text{ GeV}/c^2$, and a fixed neutralino mass of $M_{\chi} = 25 \text{ GeV}/c^2$. The neutralino limit of $M_{\chi} = 25 \text{ GeV}/c^2$ is set at the point $(\mu, M_2) \sim (-60, 40)$ by an interplay of the LEP1 and LEP2 exclusion limits.*

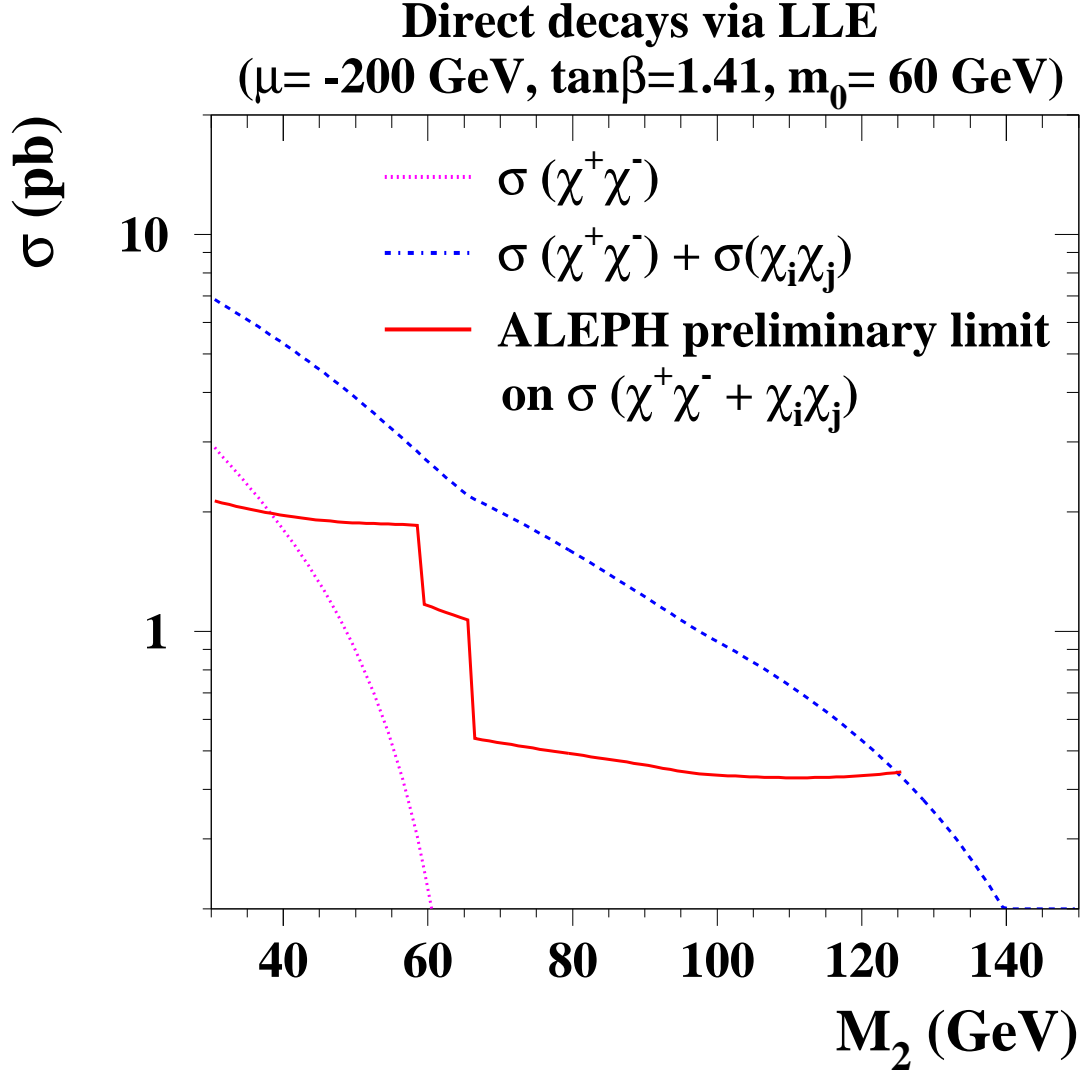


Figure 5: The solid line shows the combined excluded cross section from the chargino and neutralino searches ($\sqrt{s} = 172$ GeV) at the 95% C.L. as a function of M_2 for a dominant $LL\bar{E}$ coupling and fixed values of $\tan\beta = 1.41$, $m_0 = 60$ GeV/ c^2 , $\mu = -200$ GeV/ c^2 , assuming that the direct decays dominate. For the low value of m_0 considered here the neutralino production cross section (dashed line) is enhanced due to positive contributions from selectron t -channel exchange, and therefore the excluded region extends well beyond the kinematic limit for chargino pair production ($M_2 \lesssim 60$ GeV/ c^2).

Slepton Exclusion (at 95%CL) from $\sqrt{s}=130-172$ GeV Data

ALEPH PRELIMINARY

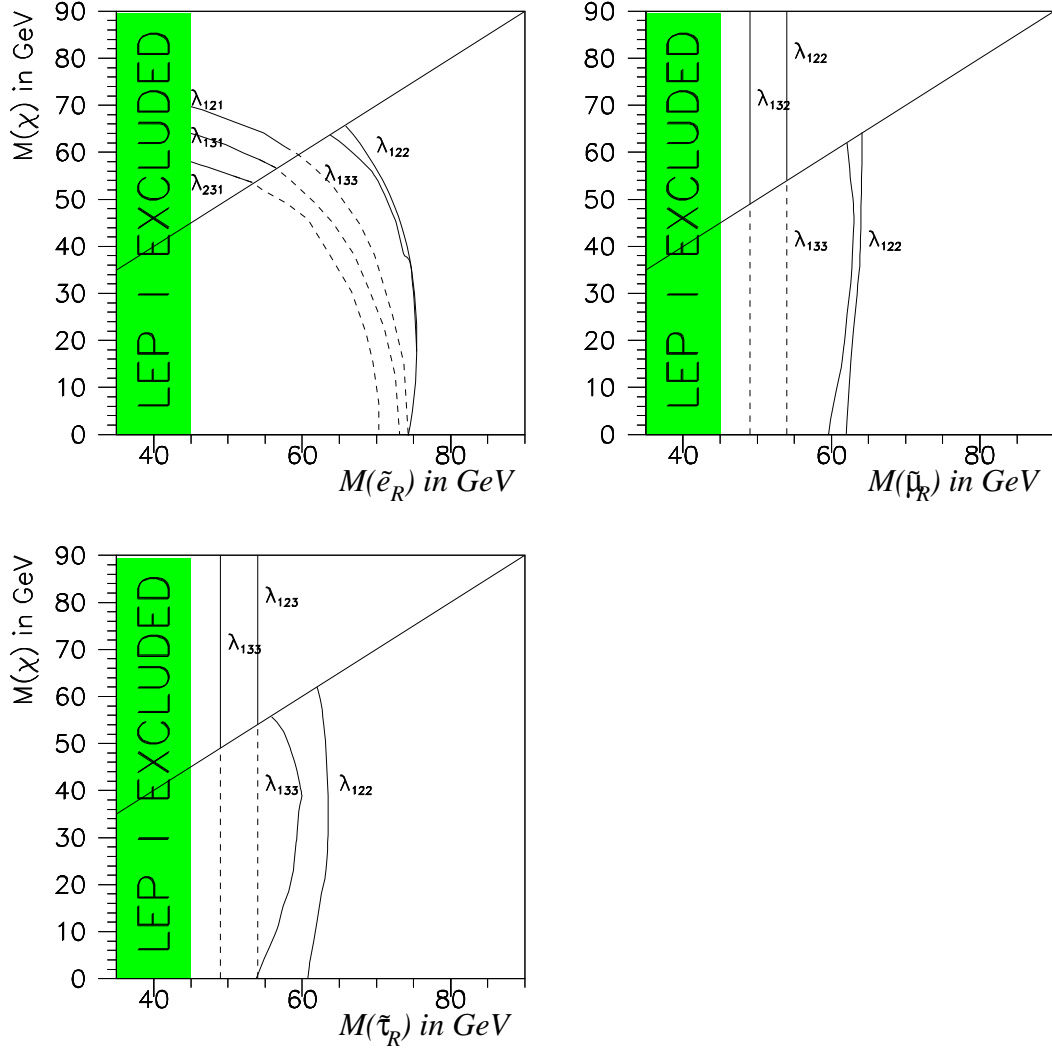


Figure 6: The 95% C.L. limits in the $(m_\chi, m_{\tilde{l}_R})$ plane for a dominant $LL\bar{E}$ coupling. Above the diagonal line the lightest neutralino is heavier than the sleptons, and only the direct decays are allowed. Below the line the indirect decays generally dominate, but the branching ratio of the direct (dashed lines) to indirect (full lines) decays depends on the magnitude of the coupling λ_{ijk} . The two choices of λ_{122} and λ_{133} correspond to the best and worst case exclusions for the indirect decays, respectively. The selectron limit is shown at a representative point in the gaugino region ($\mu = -200$ GeV/ c^2 and $\tan\beta = \sqrt{2}$).

Sneutrino Exclusion (at 95%CL) from $\sqrt{s}=130-172$ GeV Data

ALEPH PRELIMINARY

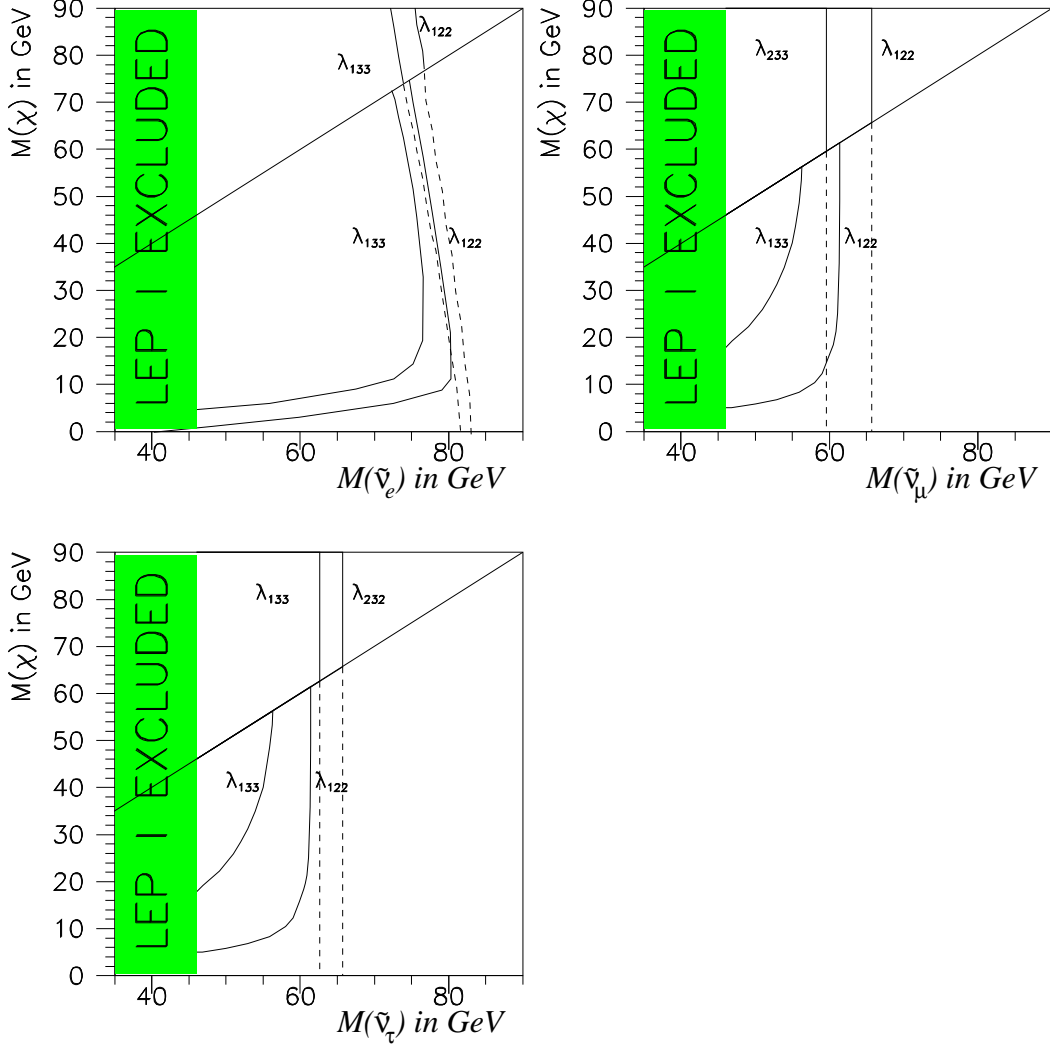


Figure 7: 95% *C.L.* limits in the $(m_\chi, m_{\tilde{\nu}})$ plane for a dominant $LL\bar{E}$ coupling. Above the diagonal line the lightest neutralino is heavier than the sneutrino and only the direct decays are allowed. Below the line the indirect decays generally dominate (full lines), but the branching ratio of the direct (dashed lines) to indirect decays depends on the magnitude of the coupling λ_{ijk} . The different choices of λ_{ijk} correspond to the best and worst case scenarios. The electron sneutrino limit is shown at a representative point in the gaugino region ($\mu = -200$ GeV/ c^2 and $\tan\beta = \sqrt{2}$).

Squark Exclusion (at 95%CL) from $\sqrt{s}=130-172$ GeV Data
ALEPH PRELIMINARY

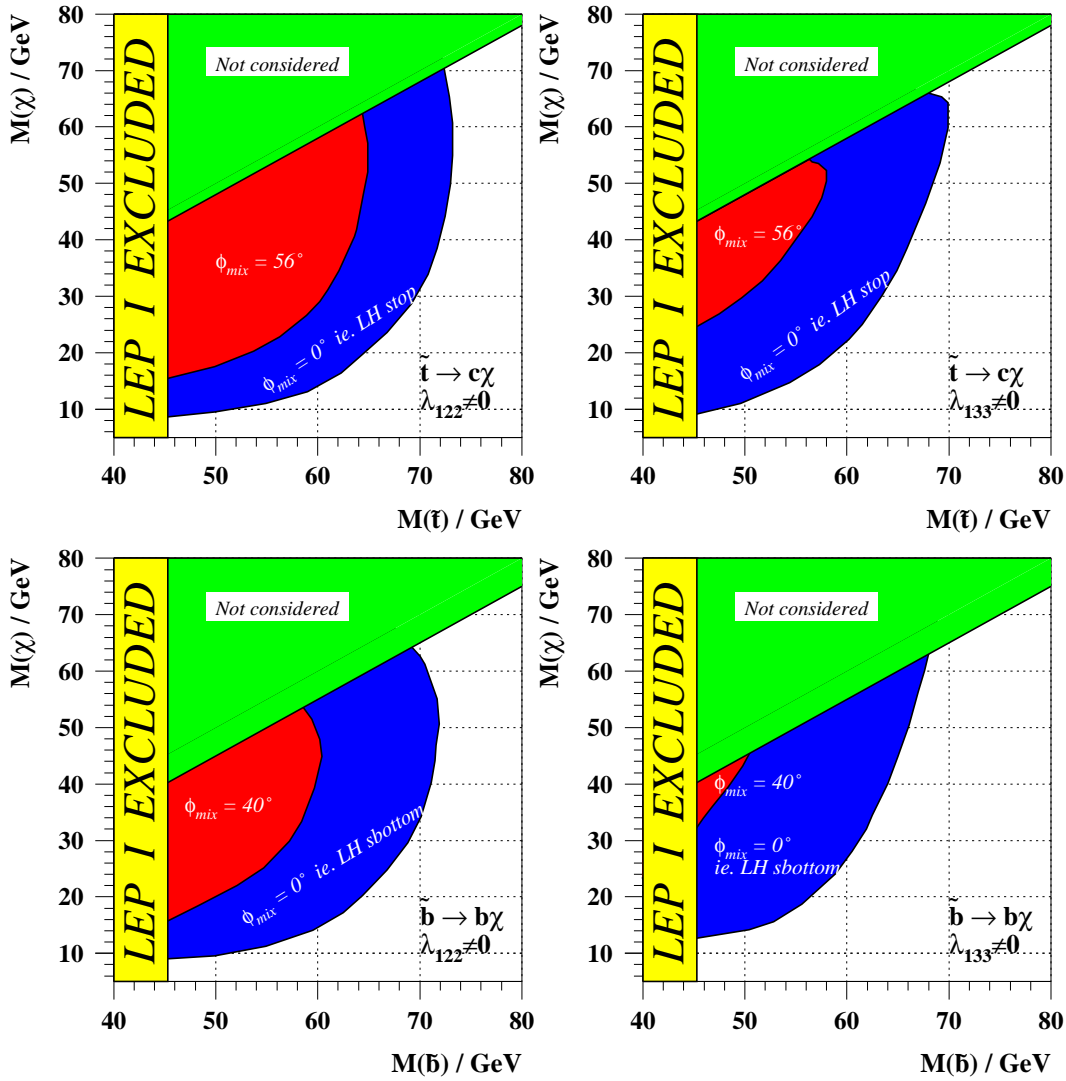


Figure 8: 95% C.L. limits on the stop and sbottom in the $(m_\chi, m_{\bar{q}})$ plane for a dominant $LL\bar{E}$ coupling. The two choices of λ_{122} and λ_{133} correspond to the best and worst case exclusions, respectively. The exclusion plots are shown for minimal squark mixing ($\theta = 0^\circ$), and for $\theta = 56^\circ, 40^\circ$ for stops and sbottoms, respectively.

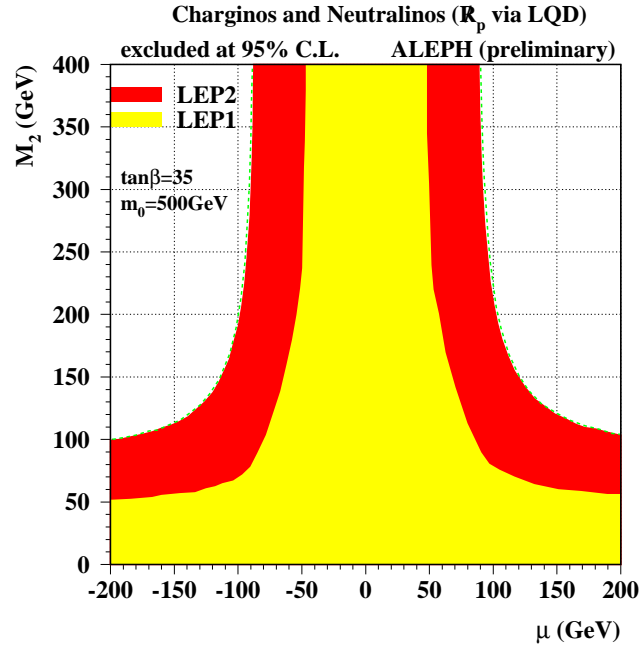
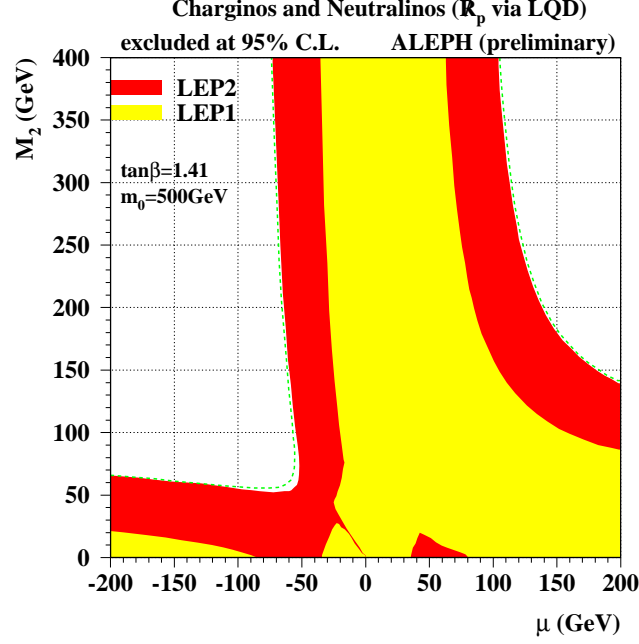


Figure 9: The $LQ\bar{D}$ chargino 95% C.L. exclusion in the (μ, M_2) plane for the two values of $\tan\beta = \sqrt{2}, 35$. The corresponding chargino mass limits are $M(\chi^+) = 83, 85 \text{ GeV}/c^2$, respectively, valid for any choice of generation indices i, j, k of the coupling λ'_{ijk} , and valid for $m_0 = 500 \text{ GeV}/c^2$, i.e. large sfermion masses.

Slepton, Sneutrino exclusion from $\sqrt{s}=130\text{-}172$ GeV Data
ALEPH preliminary

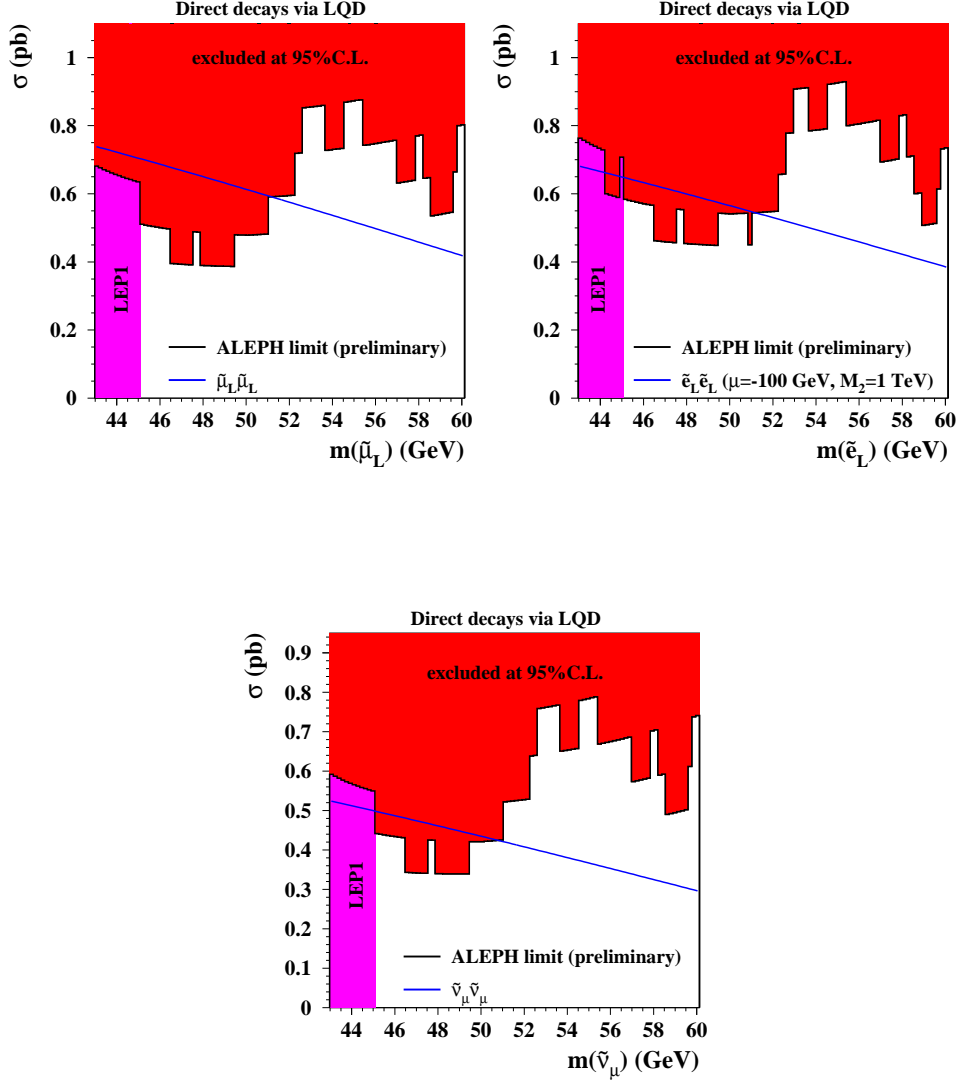


Figure 10: The dark shaded regions show the 95% C.L. excluded cross sections as a function of the slepton/sneutrino mass for the direct decays into four jets for a dominant $LQ\bar{D}$ coupling. The superimposed lines show the predicted cross sections for slepton and sneutrino pair production. The mass limits are set at $M(\tilde{\mu}_L, \tilde{\tau}_L) > 51$ GeV/ c^2 , for selectrons at $M(\tilde{e}_L) > 51$ GeV/ c^2 in the deep higgsino region ($\mu = -100$ GeV/ c^2 , $M_2 = 1$ TeV/ c^2), and for sneutrinos (one flavour) at $M(\tilde{\nu}) > 51$ GeV/ c^2 , valid for any choice of generation indices i, j, k of the coupling λ'_{ijk} .

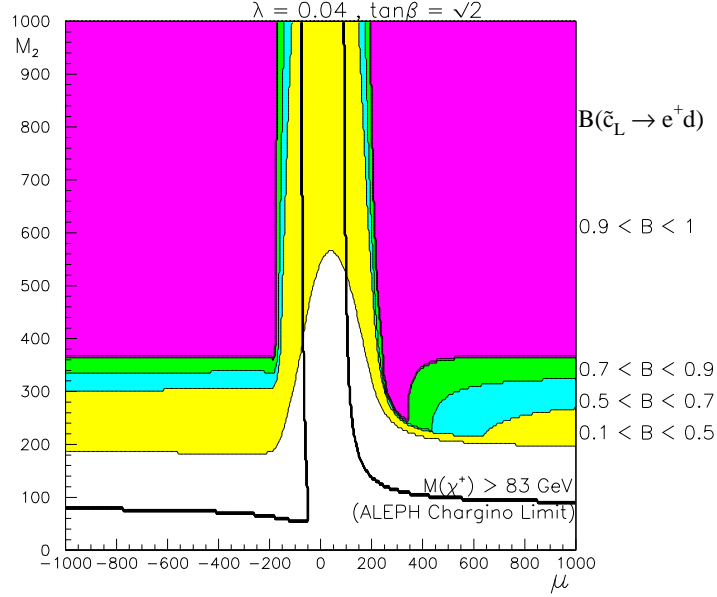


Figure 11: The hatched regions show contours of $B(\tilde{c}_L \rightarrow e^+ d)$ for the HERA solution $\lambda'_{121} = 0.04$, $M_{\tilde{c}_L} = 200 \text{ GeV}/c^2$ at $\tan \beta = \sqrt{2}$. The plot is to be compared with Fig.4 of [22]. Regions with $B > 0.87$ are excluded by the Tevatron searches [21]. On the other hand, if $B \ll 1$, the coupling λ'_{121} would have to be increased correspondingly to ($\lambda'_{121} = 0.04/\sqrt{B}$) to account for the HERA high Q^2 excess, and be in conflict with low energy bounds. The ALEPH chargino limit, $M_{\chi^+} > 83 \text{ GeV}/c^2$, is shown as a solid line.

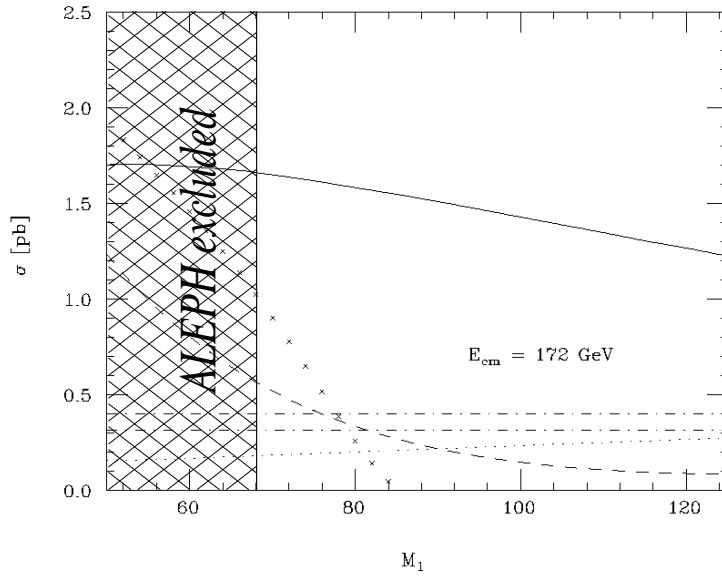


Figure 12: The plot, taken from reference [10], shows the theoretical cross sections for: $\tilde{e}_L \tilde{e}_R$ (solid lines), $\tilde{e}_L \tilde{e}_L$ (dotted lines), $\tilde{e}_R \tilde{e}_R$ (dashed lines), $\tilde{\nu} \tilde{\nu}$ (dot-dashed lines), and $\chi \chi$ (crosses) as a function of the $U(1)$ gaugino mass M_1 , for $M_{\tilde{e}_L} = 58 \text{ GeV}/c^2$ and $M_{\tilde{e}_R} = 48 \text{ GeV}/c^2$. The crossed region shows the excluded region for $\tilde{e}_R \tilde{e}_R$ production ($\sigma_{\text{ex}} \sim 0.55 \text{ pb}$) by the four jet analysis of Section 3.2.2.